

## Non-conventional magnetic order in Fe-substituted $\text{La}_{0.7}\text{Sr}_{0.3}\text{MnO}_3$ giant-magnetoresistance manganites

This article has been downloaded from IOPscience. Please scroll down to see the full text article.

2002 J. Phys.: Condens. Matter 14 12563

(<http://iopscience.iop.org/0953-8984/14/47/328>)

View [the table of contents for this issue](#), or go to the [journal homepage](#) for more

Download details:

IP Address: 171.66.16.97

The article was downloaded on 18/05/2010 at 19:11

Please note that [terms and conditions apply](#).

# Non-conventional magnetic order in Fe-substituted $\text{La}_{0.7}\text{Sr}_{0.3}\text{MnO}_3$ giant-magnetoresistance manganites

J M Barandiarán<sup>1,3</sup>, J M Greneche<sup>2</sup>, T Hernández<sup>1</sup>, F Plazaola<sup>1</sup> and T Rojo<sup>1</sup>

<sup>1</sup> Universidad del País Vasco UPV/EHU, Facultad de Ciencias y Unidad Asociada al CSIC, PO Box 644, E-48080 Bilbao, Spain

<sup>2</sup> Laboratoire de Physique de L'Etat Condensé UMR CNRS 6087, Université du Maine, 72085 Le Mans, France

E-mail: manub@we.lc.ehu.es (J M Barandiarán)

Received 7 July 2002

Published 15 November 2002

Online at [stacks.iop.org/JPhysCM/14/12563](http://stacks.iop.org/JPhysCM/14/12563)

## Abstract

Magnetization measurements and Mössbauer spectrometry have been performed on  $\text{La}_{0.7}\text{Sr}_{0.3}\text{Mn}_{1-x}\text{Fe}_x\text{O}_3$  ( $x = 0.01, 0.05, 0.1, 0.2, 0.30$ ), to clarify the local magnetic order around  $\text{Fe}^{3+}$  ions. As Mn atoms are substituted for with Fe, the magnetic structure dramatically changes, because the ferromagnetic double-exchange chain is broken. At 4.2 K all compounds are magnetically ordered with large hyperfine fields. For  $x = 0.05$  ferromagnetic and paramagnetic phases coexist over a large temperature range. Magnetic ordering occurs in a double step. Superparamagnetic effects are observed, and can explain part of this atypical ordering process, but there is evidence of segregation and clustering of Fe, even at this low concentration.

(Some figures in this article are in colour only in the electronic version)

## 1. Introduction

In the last few years there has been intensive work on the competition of exchange interactions and magnetic structures in Fe-substituted giant-magnetoresistance perovskites [1–8]. These compounds are prepared by traditional ceramic methods or, more recently, by a softer sol–gel method. They have compositions such as  $\text{Ln}_{0.7}\text{M}_{0.3}\text{MnO}_3$ , where Ln is a lanthanide and M is a divalent cation (Ca, Sr, Ba, Pb, etc). When Mn is partially substituted for with Fe the compounds show a clear competition between the Fe–Mn (antiferromagnetic) and the Mn–Mn (ferromagnetic) exchange interactions [1–8]. The ferromagnetic character of the unsubstituted manganites is mainly due to double exchange between  $\text{Mn}^{3+}$  and  $\text{Mn}^{4+}$  ions [8–11]. This fluctuating valence of Mn ions also gives rise to a delocalized electron that accounts for the

<sup>3</sup> Author to whom any correspondence should be addressed.

metallic character of the magnetically ordered compounds. As the Mn atoms are substituted for with Fe the magnetic structure dramatically changes: the larger the Fe content, the lower the Curie temperature and the magnetic moment per Mn/Fe atom, because the ferromagnetic double-exchange chain is broken, Fe entering always as  $\text{Fe}^{3+}$  ions in the compounds [1–4]. Also the metallic character disappears in this process. At large Fe concentrations (typically above 20%, i.e. at the percolation limit) spin-glass-like structures have been reported (see below) but there is no clear evidence of the exact magnetic structure of the compounds. This could also be due to mictomagnetic local structures arising from frustration, as a consequence of the different kinds of exchange interaction. Phase separation has been strongly suggested even in the absence of Fe doping [12, 13].

More recently, double perovskites of composition  $\text{Sr}_2\text{FeMO}_6$  ( $M = \text{Mo}, \text{Re}, \text{etc}$ ) have been studied [14–16]. These compounds might show structural order for the Fe/M sites in a NaCl structure accompanied by half-metallic ferromagnetism up to elevated temperatures (415 K for  $\text{Sr}_2\text{FeMoO}_6$ ). Large changes in the order, both magnetic and structural, have been found upon small substitutions of other metals for Fe and M. In this case it seems that a similar double-exchange mechanism occurs and the magnetic order and moment are intimately related to the cation order, which can be increased or decreased upon such substitutions.

A microscopic local study seems then interesting in order to clarify the nature of the magnetic interactions and structures of these compounds.

In this work, we present a study based on magnetization measurements and Mössbauer spectrometry performed on  $\text{La}_{0.7}\text{Sr}_{0.3}\text{Mn}_{1-x}\text{Fe}_x\text{O}_3$  ( $x = 0.01, 0.05, 0.1, 0.2, 0.30$ ), in an attempt to clarify both the magnetic behaviour and the local magnetic order around Fe ions. Some studies already exist on similar magnetic systems [1, 3, 4] but the amount of Fe substitution has been kept below  $x = 0.1$ , thus giving a partial vision of the role of magnetic interactions.

## 2. Experimental procedure

The compounds were prepared by traditional solid-state reaction in air, starting with  $^{57}\text{Fe}$ -enriched  $\text{Fe}_2\text{O}_3$ , in order to have enough Mössbauer absorption, even at the lowest doping levels. X-ray patterns were obtained using a Philipps X'PERT diffractometer using  $\text{Cu K}\alpha$  radiation and then analysed by means of FULLPROF refinement software [17]. Magnetic measurements were carried out in a 7 T SQUID magnetometer at the Magnetic Measurements Service of the University of the Basque Country, while transmission Mössbauer spectra were recorded using a constant-acceleration spectrometer with a  $^{57}\text{Co}$  source diffused into a Rh matrix. The powdered sample was cooled in a bath cryostat and some in-field Mössbauer spectra were recorded either at room temperature under a small magnetic field oriented perpendicular to the  $\gamma$ -radiation or at low temperature using a cryomagnetic device where the external magnetic field is parallel to the  $\gamma$ -radiation. The hyperfine parameters are refined by means of the MOSFIT program [18] while the values of the isomer shift are quoted relative to that of  $\alpha$ -Fe at 300 K.

## 3. Results and discussion

### 3.1. Magnetic measurements

Some structural results on the same samples have already been reported in [8]. In summary, all these single-phase compounds exhibit rhombohedral structure with space group  $R\bar{3}c$ . The lattice parameters remain almost unchanged upon substitution of Fe for Mn and only a slight

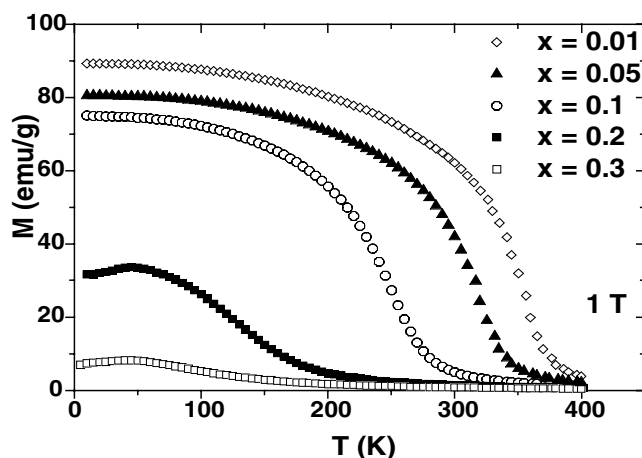


**Figure 1.** Magnetization as a function of temperature for all the  $\text{La}_{0.7}\text{Sr}_{0.3}\text{Mn}_{1-x}\text{Fe}_x\text{O}_3$  samples studied. The applied field was 1 T.

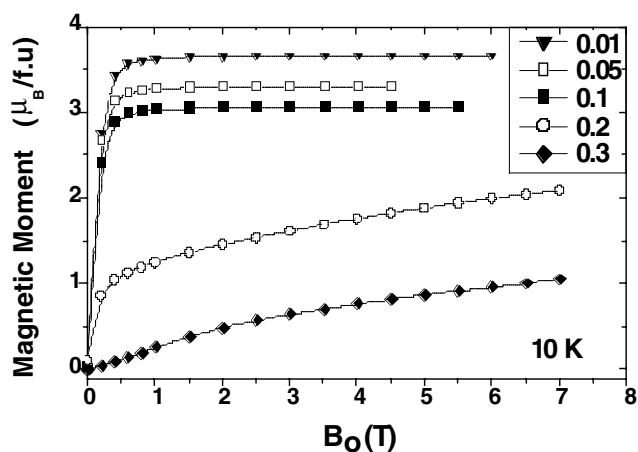


**Figure 2.** Magnetization curves as a function of the applied field at 10 K for all compounds. Note the lack of saturation for the  $x = 0.2$  and  $0.3$  samples.

increase in the cell volume (from  $351.7$  up to  $352.6 \text{ \AA}^3$ ) was observed. This is consistent with the ionic radius of the Fe being only slightly larger than that of Mn. On the other hand, Mössbauer spectra taken in the paramagnetic region indicate an increasing distortion of the oxygen octahedral unit (as deduced from the increase of the quadrupolar splitting) around Fe with increasing doping content. This can be explained by the increase of Fe nearest-neighbour disorder with the Fe content.

From a magnetic point of view, both the Curie temperature and the magnetic moment of the compounds decrease with the Fe content, but the general, macroscopic, magnetization versus temperature curves are all similar up to  $x = 0.1$ . However, a transition is clear for  $x = 0.2$  and  $0.3$  with a maximum in the magnetization curve obtained at 1 T (figure 1). Magnetization as a function of field at 10 K (figure 2) shows a further difference between the  $x = 0.2$  and  $0.3$  compounds. The first one still has some spontaneous magnetization, as extrapolated (Arrott

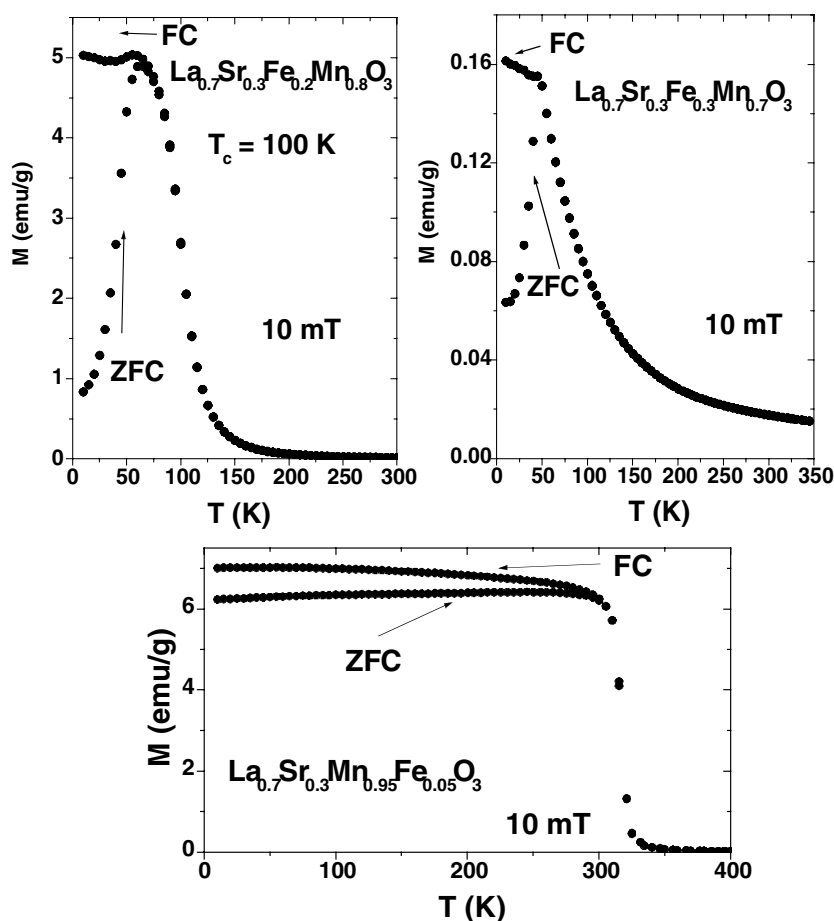


**Figure 3.** ZFC–FC curves for selected compositions. The applied field was 0.01 T. Highly inhomogeneous magnetic structure is evident for the  $x = 0.2$  and  $0.3$  samples. For  $x = 0.2$  it is still possible to define a Curie temperature. This is not the case for  $x = 0.3$ .

plots) from high field, while the  $x = 0.3$  compound shows no spontaneous magnetization at all. Saturation is not reached at 7 T either for  $x = 0.2$  or for  $0.3$ . The zero-field-cooling (ZFC)–field cooling (FC) curves (figure 3) indicate a large inhomogeneity of the magnetic distribution for  $x > 0.2$ , with spin-glass-like or cluster-glass-like features, in contrast to a rather homogeneous (but still not completely) behaviour for  $x = 0.05$ . From these curves we can take  $x = 0.2$  as a limiting case where spontaneous magnetization coexists with disordered, short-range-only, magnetic structures.

### 3.2. Low-temperature Mössbauer spectrometry

A better insight into the local order can be provided by Mössbauer spectrometry. The spectra of all compounds at 77 K are displayed in figure 4, but no direct comparison is possible, because at this temperature some of them are magnetically well ordered while others are still paramagnetic, or very close to paramagnetism—that with  $x = 0.2$ , for instance. The broad sextets for  $x = 0.01$ ,  $0.05$ , and  $0.1$  are surprising since the Curie temperatures of these

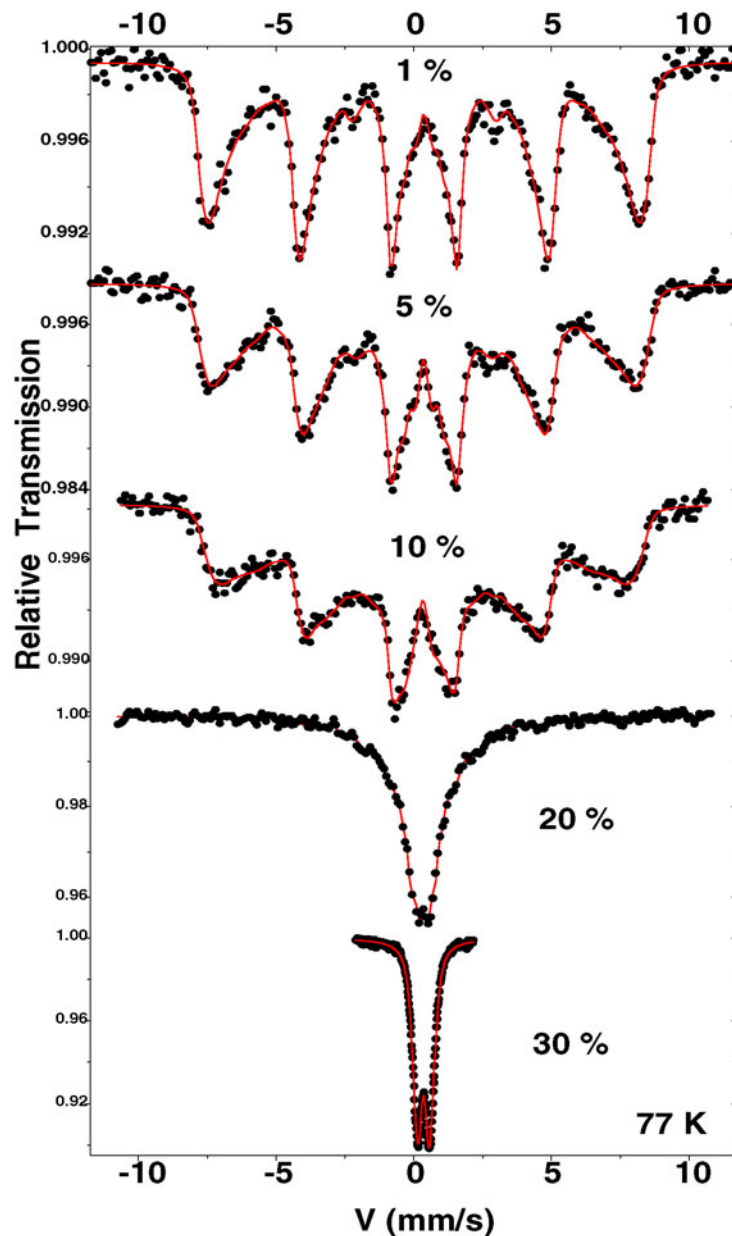


**Figure 4.** Mössbauer spectra for all compositions at 77 K. The different magnetic states of the samples are evident. Note also the broad hyperfine field distributions in the magnetically ordered samples. Fe content is indicated in at.%.

compounds are well above 250 K. This could suggest a large magnetic inhomogeneity of the Fe sites that is not revealed by macroscopic magnetization measurements. More appropriate for comparison are the spectra recorded at 4.2 K (figure 5). They show all compounds magnetically ordered with large hyperfine fields (around 50 T). A single narrow sextet accounts for the spectra of the 1% Fe-doped compound, while this sextet plus a distribution must be used to fit 5% and

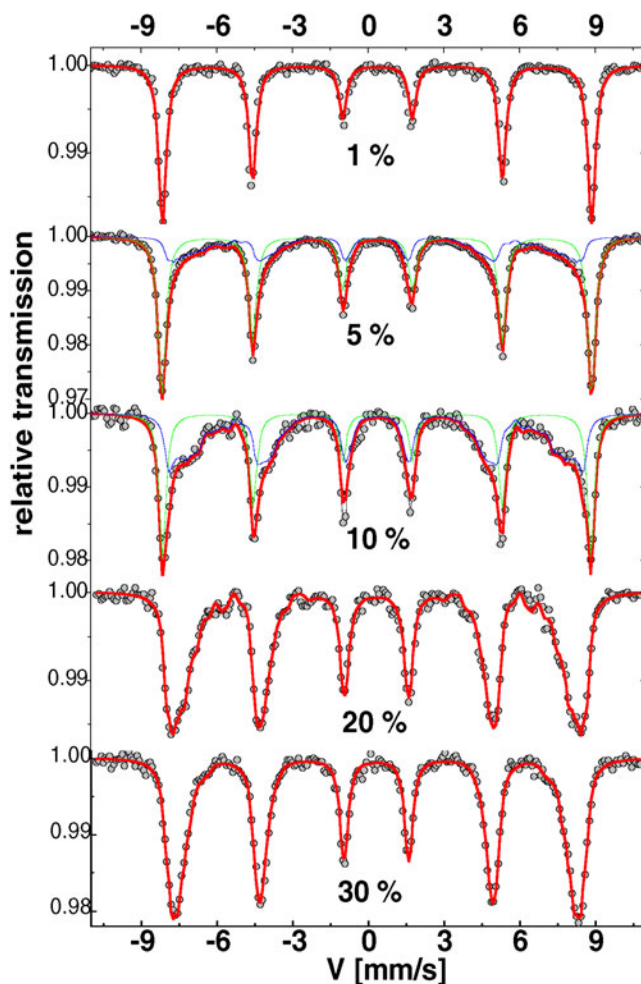


**Figure 5.** Mössbauer spectra for all compositions at 4.2 K. All samples are magnetically ordered. The existence of a discrete Fe site is evident for the  $x = 0.01, 0.05,$  and  $0.1$  samples. Broad hyperfine field distributions are found for all samples except that with  $x = 0.01$ .

10% Fe-doped ones. In the high-Fe-concentration range, the narrow sextet has disappeared and only a distribution of hyperfine fields is evident. The refined values resulting from the fitting procedure are listed in table 1. The compound with  $x = 0.2$  shows the largest distribution width, thus reflecting the intermediate magnetic behaviour.

A simple interpretation of the components of the spectra can be outlined as follows: the narrow sextet is attributed to isolated Fe ions completely surrounded by Mn. This gives a picture of the undoped compound and corresponds well to  $\text{Fe}^{3+}$ . The broad-line component reflects the disordered  $\text{Fe}^{3+}$  and  $\text{Mn}^{3+}$  neighbouring  $\text{Fe}^{3+}$  probes. At both 5% and 10% Fe concentrations, the two components thus coexist, while the narrow component disappears when the Fe content is larger than 20%. That is consistent with a broad variety of cationic neighbourings of Fe. At this stage the unperturbed ferromagnetic Mn lattice no longer exists.

The above fitting procedure is only a rough attempt to describe the situation. More elaborate strategies can be envisaged using single components, each one related to a given

**Table 1.** Hyperfine parameters for all compounds at 4.2 K. IS = isomer shift,  $\Gamma$  = linewidth,  $2\varepsilon$  = quadrupole shift,  $B_{\text{HF}}$  = hyperfine field of a single sextet (s) or the average of those for a distribution (d). The relative amount of each subspectrum (last column) is deduced from the resonant areas and may be influenced by different recoilless factors.

Fe (at.%)	IS (mm s <sup>-1</sup> )	$\Gamma$ (mm s <sup>-1</sup> )	$2\varepsilon$ (mm s <sup>-1</sup> )	$B_{\text{HF}}$ (T)	(%)
	$\pm 0.02$	$\pm 0.02$	$\pm 0.02$	$\pm 0.5$	$\pm 2$
1	0.50	0.37	-0.02	52.6 (s)	100
5	0.50	0.36	-0.03	52.7 (s)	67
	0.45	—	0.06	45.4 (d)	33
10	0.50	0.34	-0.04	52.5 (s)	42
	0.48	—	-0.06	46.0 (d)	58
20	0.48	—	0.01	48.0 (d)	100
30	0.47	—	-0.01	48.6 (d)	100

number of Fe–Mn neighbours. In fact a discrete sextet with  $B_{\text{HF}} = 51.2$  T can be separated in the spectra corresponding to  $x = 0.05$  and 0.1. This sextet should correspond to the Fe sites with five Mn and one Fe nearest neighbours in the otherwise undoped Mn matrix, which have a small but non-negligible probability of existing. Higher numbers of Fe neighbours, however, have different contributions depending on their exact position in the six nearest-neighbour sites, and will give rise to a great number of hyperfine contributions.

The probability of random states with one or more Fe as nearest neighbours (binomial distribution) in the compounds with  $x = 0.05$  and 0.1 (about 26 and 47% respectively) is smaller than the experimentally observed ratio between the distribution of  $B_{\text{HF}}$  and the narrow sextet (see table 1). This can be taken as an indication of the existence of some segregation of phases, corresponding to the inhomogeneity in the Fe surroundings, at least from the magnetic point of view, in accordance with the previous ideas derived from the broad spectra at 77 K. That point can be further investigated by following the temperature behaviour of the Mössbauer spectra.

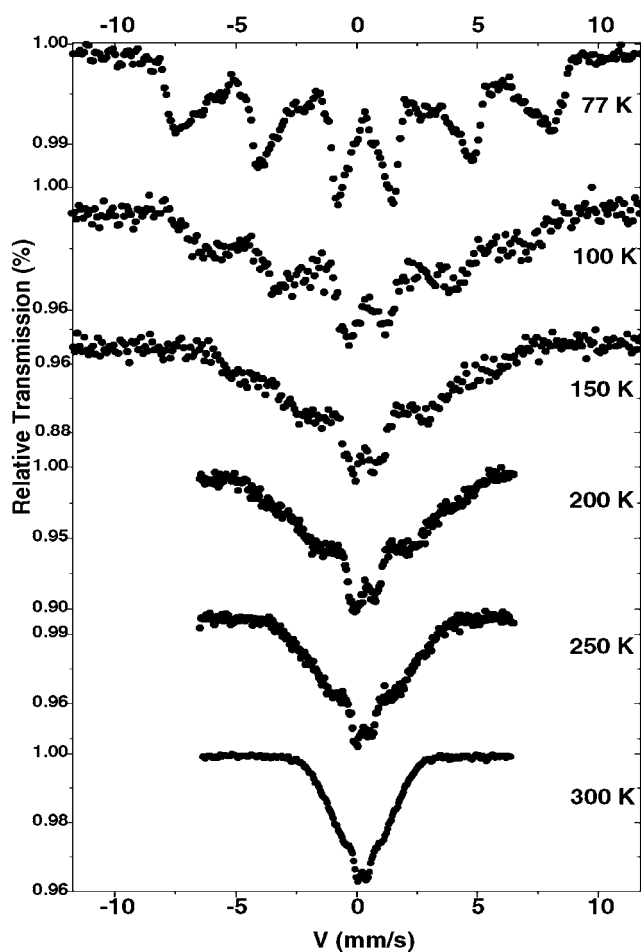
### 3.3. Temperature-dependent Mössbauer spectrometry

Figure 6 shows the evolution of the spectra as a function of temperature for the compound with  $x = 0.05$ , which has the highest Curie temperature, but is already showing the broad distribution of  $B_{\text{HF}}$  at 4.2 K. It can be seen that the paramagnetic–ferromagnetic transition develops progressively and extends over the temperature range studied. From previous high-temperature measurements [8], we know the paramagnetic spectrum of this compound. The paramagnetic spectra were subtracted, with a different weight in each case, from those in figure 6, in order to obtain the contributions of magnetically ordered and disordered phases present at each temperature. A large distribution of hyperfine fields is found in the ordered phase for all study temperatures, down to 77 K. Figure 7 represents the relative amounts of paramagnetic and ordered phase as a function of temperature. It is clear that the coexistence of the two phases follows a double-step evolution. First a large amount of the sample orders around room temperature and afterwards total ordering appears at much lower temperature. The evolution of the average hyperfine field of the distribution is also shown in figure 7. This can be seen as a superposition of two ferromagnetic phases with  $T_c$  at about 100 and 320 K respectively, the latter corresponding to the macroscopic  $T_c$  of the compound.

Similar experiments performed on the  $x = 0.2$  compound show only a single step in the ordering, while not enough data points were taken to fully establish this.

In the above discussion we have no a clear picture of whether the different phases involved are spatially separated and constitute real segregation of clusters or similar units,





**Figure 6.** Mössbauer spectra as a function of temperature for the  $\text{La}_{0.7}\text{Sr}_{0.3}\text{Mn}_{0.95}\text{Fe}_{0.05}\text{O}_3$  sample. Both ferromagnetic (with broad hyperfine field distribution) and paramagnetic contributions are needed for fitting the spectra over the whole temperature range.

having different compositions on average, or the random distribution of Fe atoms gives rise to different local magnetic states in an overall homogeneous sample. In either case the sizes and characteristics of these zones are unknown. On the other hand, dynamic magnetization effects, such as superparamagnetism, can greatly influence the magnetization and hyperfine field. Because x-ray patterns do not reveal any ultrafine crystalline grains, dynamic effects give rise to the overall appearance of the existence of different magnetic phases, while only a distribution of magnetic cluster sizes, with different blocking temperatures, is present. New experiments are thus needed to clarify these possibilities.

### 3.4. Mössbauer spectrometry under an applied magnetic field

Evidence of possible dynamic effects of the magnetization can be easily obtained in  $^{57}\text{Fe}$  Mössbauer spectrometry by the application of an external magnetic field. Should superparamagnetic relaxation be responsible for a collapse of the hyperfine field, the application

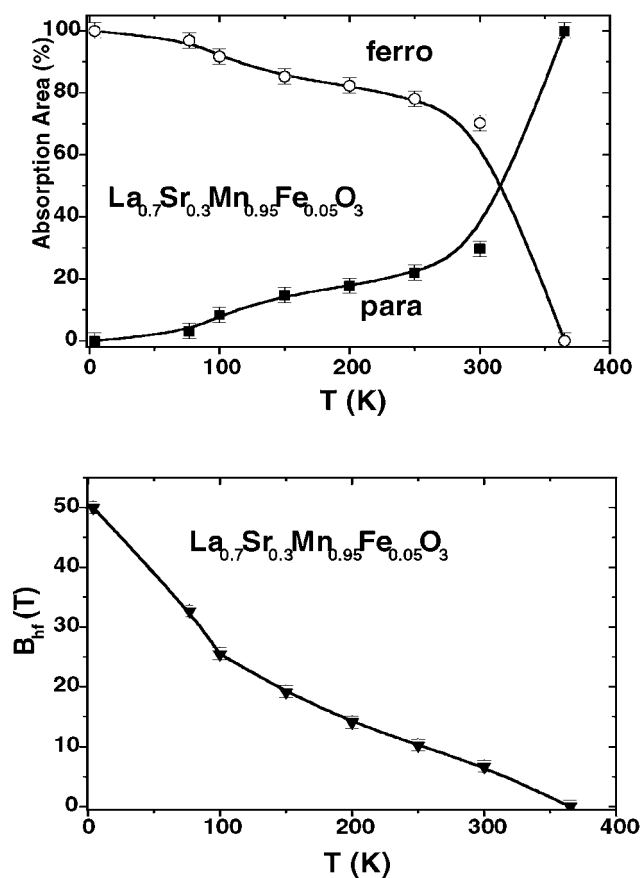


**Figure 7.** Evolution of the relative amounts of paramagnetic and ferromagnetic phase (upper part) and average hyperfine field (lower part) as a function of temperature in  $\text{La}_{0.7}\text{Sr}_{0.3}\text{Mn}_{0.95}\text{Fe}_{0.05}\text{O}_3$ . Solid lines are only guides for the eyes. The two-step ordering process commented on in the text is evident.

of a small field can be enough to block the magnetic moments, and a large increase of the hyperfine field, or an increase of the resonant area corresponding to magnetically ordered states, should be obtained. On the other hand, the existence of magnetic clusters with different compositions, and having different Curie temperatures, will give rise to almost unchanged spectra if the applied field is not of the order of the internal hyperfine field of the clusters. In order to explore the effect of the field we choose the compound with  $x = 0.05$ , which has more complicated features.

The first experiments under an applied field were performed at room temperature and in a field of about 0.1 T. At this temperature the compound is close to the Curie temperature and about 30% of the sample is still paramagnetic. Despite the lack of resolution of the hyperfine structure, the influence of the field is rather clear and the fitting procedure for the spectra is consistent with a reduction of the paramagnetic phase to about 15% of the total absorption, with no change in the hyperfine parameters. The existence of dynamic effects is then clear, although the total volume of the sample is not driven to ferromagnetism by the applied field at this high temperature, i.e. there is still some area in the spectrum that corresponds to a paramagnetic state. This could be because the small field applied is not enough to overcome

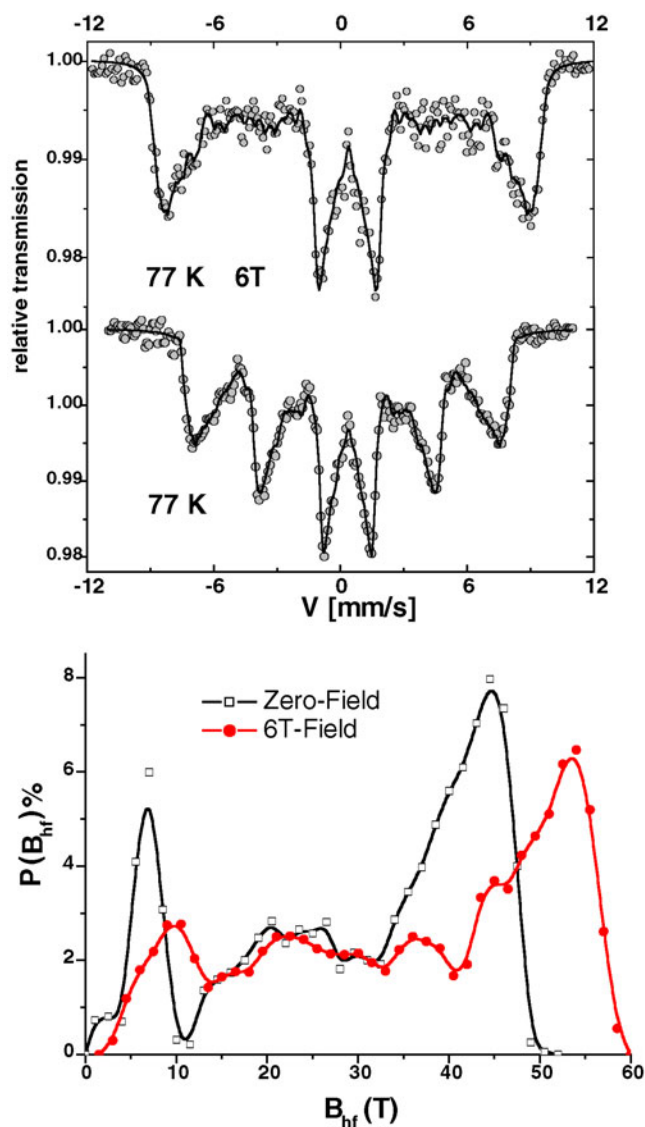


**Figure 8.** The effect of a strong magnetic field (6 T) on the Mössbauer spectra at 77 K for  $\text{La}_{0.7}\text{Sr}_{0.3}\text{Mn}_{0.95}\text{Fe}_{0.05}\text{O}_3$ , and associated hyperfine field distributions. The low-field part of the distribution (below 10 T) is due to the superparamagnetic or true paramagnetic clusters. The blocking process for the superparamagnetic states and the shift of the high-field part of the distribution are commented on in the text.

the temperature effect on the smallest superparamagnetic zones, or because some clusters that are still in a true paramagnetic state exist.

Further experiments were carried out at 77 K in the presence of a strong magnetic field of 6 T, oriented parallel to the incident gamma radiation. As is shown in figure 8, the almost complete disappearance of lines 2 and 5 of the spectrum and the increase of the hyperfine field in the external lines (1 and 6) clearly indicates a rather collinear magnetic structure with the Fe magnetic moment anti-parallel to the mean magnetization in the sample. Indeed, the

mean effective field is about 5 T larger than the mean hyperfine field, whereas the main peak is shifted by about 7 T and the low-field peak disappears upon applying external field. This confirms the antiferromagnetic Fe–Mn coupling and the occurrence of superparamagnetic clusters suggested in the previous section. Such features were already observed in the case of iron-doped  $\text{La}_{0.75}\text{Ca}_{0.25}\text{MnFeO}_3$  [3]. In addition, the paramagnetic component is halved, as in the room temperature experiments, and all the hyperfine field distribution is shifted to high fields. However, at this temperature (77 K) the decrease of the paramagnetic component of the spectrum is already achieved in a much smaller field of about 0.04 T, without producing changes in the hyperfine parameters. Once again the complete magnetic ordering of Fe is not accomplished even in a large field and at low temperature.

By comparing the broad distribution of hyperfine fields at 77 K for the sample with 5% Fe with the distributions found in the 20 and 30% Fe compounds, and the very similar ordering temperatures, we can deduce that the structure of the clusters is itself chemically ( $\text{Fe}^{3+}$  and  $\text{Mn}^{3+/4+}$ ) highly disordered and magnetically non-collinear.

#### 4. Conclusions

It is concluded that the  $^{57}\text{Fe}$  Mössbauer effect is able to give insight into the local magnetic order in these compounds more specifically than macroscopic magnetic measurements, dominated by the effect of the magnetization of Mn, and that, although dynamic effects can explain part of the atypical magnetic ordering process in Fe-doped manganites, there is evidence of segregation and clustering of the Fe, even at low concentrations. The magnetic structure of the clusters is similar to that of the high-concentration Fe compounds, which show high magnetic disorder at the microscopic level.

#### References

- [1] Leung L K, Morrish A H and Evans B J 1976 *Phys. Rev. B* **13** 4069
- [2] Gutiérrez J, Peña A, Barandiarán J M, Pizarro J L, Hernández T, Lezama L, Insausti M and Rojo T 2000 *Phys. Rev. B* **61** 9028
- [3] Hannoyer B, Marest G, Greneche J M, Bathe R, Patil S I and Ogale S B 2000 *Phys. Rev. B* **61** 9613
- [4] Simopoulos A, Pissas M, Kallias G, Devlin E, Moutis N, Panagiotopoulos I, Niarchos D, Christides C and Sonntag R 1999 *Phys. Rev. B* **59** 1263
- [5] Ahn K H, Wu X W, Liu K and Chien C L 1997 *J. Appl. Phys.* **15** 5505
- [6] Righi L, Gorria P, Insausti M, Gutiérrez J and Barandiarán J M 1997 *J. Appl. Phys.* **81** 5767
- [7] Pissas M, Kallias G, Devlin E, Simopoulos A and Niarchos D 1997 *J. Appl. Phys.* **81** 5770
- [8] Hernández T, Plazaola F, Rojo T and Barandiarán J M 2001 *J. Alloys Compounds* **323/324** 440
- [9] Zener C 1951 *Phys. Rev.* **82** 403
- [10] Goodenough J B 1955 *Phys. Rev.* **100** 564  
Goodenough J B and Zhou J-S 1997 *Nature* **386** 229
- [11] de Gennes P G 1960 *Phys. Rev.* **118** 141
- [12] Uehara M, Mori S, Chen C H and Cheong S-W 1999 *Nature* **399** 560
- [13] Moreo A, Yunoki S and Dagotto E 1999 *Science* **283** 2034
- [14] Kobayashi K I, Kimura T, Sawada H, Terakura K and Tokura Y 1998 *Nature* **395** 677
- [15] Blanco J J, Hernández T, Rodríguez-Martínez L M, Insausti M, Barandiarán J M, Greneche J M and Rojo T 2001 *J. Mater. Chem.* **11** 253
- [16] Greneche J M, Venkatesan M, Suryanarayanan R and Coey J M D 2001 *Phys. Rev. B* **63** 174403
- [17] Rodríguez-Carvajal J 1990 *FULLPROF Program, Rietveld Pattern Matching Analysis of Powder Patterns* ILL, Grenoble
- [18] Teillet J and Greneche J M, *MOSFIT Program* University of Le Mans, unpublished